1986

Performance Analysis of Scroll Compressor for Air Conditioners

S. Nagatoma

H. Sakata

M. Hayano

M. Hatori

PERFORMANCE ANALYSIS OF SCROLL COMPRESSOR FOR AIR CONDITIONERS

Makoto Hayano, Shigemi Nagatomo, Hirotsugu Sakata and Mitsuo Hatori

Household Appliances Engineering Laboratory,
Toshiba Corporation, Yokohama City, Japan

ABSTRACT

In this study, a series of semi-circles were employed for the scroll walls. The compression process was investigated geometrically, and then the forces acting on the orbiting scroll were calculated. By using this analysis, the original method, which utilizes high pressure against the thrust force acting on the orbiting scroll, was suggested. Further, the prototype was developed, and its performance was investigated experimentally.

The results of these investigations can be summarized as follows:

(1) The basic equations for the compression chamber volume, the forces acting on the orbiting scroll were obtained in the case in which a series of semi-circles were utilized for the scroll walls.

(2) It has been clarified that the original method, which utilizes the discharge pressure against the thrust force, is practical.

(3) By improving the axial and radial clearances in wrap to be optimum and by using the above-mentioned method, the prototype of the scroll compressor, which has high overall efficiency and high volumetric efficiency, has been developed.

INTRODUCTION

Recently, scroll compressors are being studied and developed because of their special features of (a) high efficiency, (b) low noise and vibration, (c) small size, and (d) light weight. It is necessary to find

the forces acting on each part of the scroll compressors in order to improve their efficiency. Some theoretical studies on scroll compressors have been reported[1),(2)]. In these compressors, an involute is usually employed for the scroll walls, but a series of semi-circles is not.

So, in this study, a series of semi-circles is employed. The compression process is investigated geometrically, and the forces acting on the orbiting scroll are calculated. Using this calculation, the original method, which utilizes the high pressure against the thrust force acting on the orbiting scroll, is suggested.

Further, the prototype of the scroll compressor is developed, and experimental investigations have been made. The effects of the above-mentioned high pressure, axial and radial clearances in scroll wrap on the performance of this prototype have been clarified.

VOLUME AND PRESSURE OF COMPRESSION CHAMBER

The volume of the compression chamber, $Vi(\theta)$, is given by

$$Vi(\theta) = 2 \cdot Ai(\theta) \cdot H \tag{1}$$

where θ is the crank angle, H is the scroll height, i means the i-th chamber from outside, and $Ai(\theta)$ is the shaded area shown in Fig.1(a) and (b). When the number of scrolls is n rolls (multiple of 0.5, i.e. n=0.5, 1, 1.5$\cdots$) plus θ_o rad. ($\theta_o < \pi$), $Ai(\theta)$ is given by

$$\begin{cases} Ai(\theta) = \frac{1}{2}[R_j^2\theta' - (R_{j-1}+t)^2\theta' + \pi\{R_{j-1}^2 - (R_{j-2}+t)^2\} \\ \qquad + R_{j-2}^2\theta'' - (R_{j-3}+t)^2\theta''], \qquad (R_{j-3} \neq R_1) \\ Ai(\theta) = \frac{1}{2}[R_j^2\theta' - (R_{j-1}+t)^2\theta' + \pi\{R_{j-1}^2 - (R_{j-2}+t)^2\} \\ \qquad + R_{j-2}^2\theta'' - R_{j-3}^2\theta''], \qquad (R_{j-3} = R_1) \end{cases} \tag{2}$$

where R is the radius of semi-circles, j means the j-th semi-circle from inside (see Fig.2), and t is the scroll thickness.

Rj in Eq. (2) is given by

$$\begin{cases} Rj = Rs + \frac{t}{2} + (j-1)(Rs+t) & (j \neq 1) \\ Rj = \frac{t}{2} & (j=1) \end{cases} \tag{3}$$

where Rs is the orbiting radius.

θ', θ'' and j in Eq.(2) are given by

$$\begin{cases} \theta' = \phi_o - \theta \\ \theta'' = \pi - \phi_o + 0 \\ j = j_{max} - 3i + 3 \end{cases} \quad (0 \leqq \theta < \phi_o) \tag{4a}$$

$$\begin{cases} \theta' = \pi + \phi_o - \theta \\ \theta'' = \theta - \phi_o \\ j = j_{max-1} - 3i + 3 \end{cases} \quad (\phi_o \leqq \theta < \pi + \phi_o) \tag{4b}$$

$$\begin{cases} \theta' = 2\pi - \theta + \phi_o \\ \theta'' = \theta - \phi_o - \pi \\ j = j_{max-2} - 3i + 3 \end{cases} \quad (\phi_o + \pi \leqq \theta \leqq 2\pi) \tag{4c}$$

where j_{max} is given by

$$\begin{cases} j_{max} = 2n+1 & (\phi_o = 0) \\ j_{max} = 2n+2 & (\phi_o \neq 0) \end{cases}$$

When j in Eq.(2) is 3 (the compression chamber is the inmost chamber shown in Fig.3), Ai(θ) is given by

$$\begin{cases} Ai(\theta) = \frac{1}{2}[R_3^2(\pi-\theta_1) + R_2^2\theta_1 - Rs(Rs+t)\sin\theta_1 \\ \qquad -\{(R_2+t)^2 - R_2^2\}(\pi-\theta_1) - R_1^2\pi], \quad (0 \leqq \theta_1 < \pi) \\ Ai(\theta) = \frac{1}{2}[(R_2^2 - R_1^2)(2\pi-\theta_1) + Rs(Rs+t)\sin\theta_1, \quad (\pi \leqq \theta_1 \leqq 2\pi) \end{cases} \tag{6}$$

where θ_1 is the crank angle shown in Fig. 3.

The displacement volume, Vst, is obtained from Eq.(1),(2), where θ=0.

$$\begin{cases} Vst = H[R_{jmax}^2 \phi_o - (R_{jmax-1}+t)^2 \phi_o + \pi\{R_{jmax-1}^2 \\ \qquad -(R_{jmax-2}+t)^2 + R_{jmax-2}^2(\pi - H_o) - (R_{jmax-3}+t)^2 \\ \qquad (\pi - \phi_o)], \quad (\phi_o \neq 0) \\ Vst = \pi H[\{R_{jmax}^2 - (R_{jmax-1}+t)^2\} + R_{jmax-1}^2 - \\ \qquad (R_{jmax-2}+t)^2\}], \quad (\phi_o = 0) \end{cases} \tag{7}$$

The pressure of the compression chamber, Pi(θ), is obtained by assuming the polytropic process as follows.

$$P_{iabs}(\theta) = P_{sabs}\left\{\frac{Vst}{Vi(\theta)}\right\}^k \tag{8a}$$

where Ps is the suction pressure, k is the polytropic index, and abs means the absolute pressure. When the compression chamber is opened by the discharge port to the discharge gas, Eq.(8a) may be reduced to the following expression.

$$P_{iabs}(\theta) = P_{dabs} \tag{8b}$$

where Pd is the discharge pressure.

FORCES ACTING ON THE ORBITING SCROLL DUE TO THE COMPRESSION OF GAS

Thrust force

The axial force due to the compression of gas, Fct (θ), is obtained, by assuming that the pressure of the compression chamber is acting up to the center line of the scroll thickness, as follows.

$$Fct(\theta) = \sum_{i=1}^{m} \{Pi(\theta) \cdot Ati(\theta)\} + Ps \cdot Ao(\theta) \tag{9}$$

where, m is the number of compression chambers, and Ati (θ) is the shaded area shown in Fig. 4. Ati(θ) is obtained from Eq.(2) as follows.

$$\begin{aligned} Ati(\theta) = \frac{1}{2}[& (R_j+\frac{t}{2})^2\theta' - (R_{j-1}+\frac{t}{2})^2\theta' \\ & +\pi\{(R_{j-1}+\frac{t}{2})^2 - (R_{j-2}+\frac{t}{2})^2\} \\ & +(R_{j-2}+\frac{t}{2})^2\theta'' - (R_{j-3}+\frac{t}{2})^2\theta''] \end{aligned} \tag{10}$$

When the compression chamber is the inmost chamber, Ati(θ) is obtained from Eq.(6) as follows.

$$\begin{cases} Ati(\theta) = \frac{1}{2}[(R_3+\frac{t}{2})^2(\pi-\theta_1) - Rs(Rs+t)\sin\theta_1], & (0 \leqq \theta_1 < \pi) \\ Ati(\theta) = \frac{1}{2}[(R_2+\frac{t}{2})^2(2\pi-\theta_1) - R_1^2(2\pi-\theta_1) \\ \qquad +Rs(Rs+t)\sin\theta_1], & (\pi \leqq \theta_1 \leqq 2\pi) \end{cases} \tag{11}$$

A_o in Eq.(9) is the area of the suction chamber which is the shaded area shown in Fig. 5.

When the space in the housing below the end plate of the orbiting scroll is provided with discharge pressure, the upward thrust force, Ft(θ), is obtained, by assuming that the pressure of the sliding surface between the end plate of the orbiting scroll and the fixed scroll is equal to (Pd+Ps)/2, as follows.

$$Ft(\theta) = -Fct(\theta)+\frac{\pi}{4}d_d{}^2P_d-\frac{\pi}{4}(d_d{}^2-d_s{}^2)\cdot\frac{Pd+Ps}{2} \qquad (12)$$

where d_d is the diameter of the end plate of the orbiting scroll, ds is the dimater of the suction chamber shown in Fig. 5.

When the space in the housing below the end plate of the orbiting scroll is provided with suction pressure, the upward thrust force, $Ft(\theta)$, is given by

$$Ft(\theta) = -\sum_{i=1}^{m}\{Pi(\theta)\cdot Ati(\theta)\}+\{\sum_{i=1}^{m}Ati(\theta)\}\cdot Ps \qquad (13)$$

Radial force

As the radial force, $Fc(\theta)$, varies in direction, first, the x-component, $Fcx(\theta)$, and y-component, $Fcy(\theta)$ of the radial force are calculated, and then $Fc(\theta)$ is calculated.

$Fcx(\theta)$ and $Fcy(\theta)$ are obtained from the scroll compressor geometry shown in Fig. 1(a), (b) and Fig.2 as follows.

$$\begin{cases} Fcx(\theta) = (-1)^N\left[\left[\sum_{j=1}^{m}(R_{i1}+R_{i2})\{P_j(\theta)-P_{j-1}(\theta)\}\right]\right. \\ \qquad\qquad \left.+T(P_d-P_s)\right]H\sin\theta_2 \qquad (14) \\ Fcy(\theta) = (-1)^N\left[\left[\sum_{j=1}^{m}R_{i2}\{P_j(\theta)-P_{j-1}(\theta)\}\right](1-\cos\theta)\right. \\ \qquad -\left[\sum_{j=1}^{m}R_{i1}\{P_j(\theta)-P_{j-1}(\theta)\}\right](1+\cos\theta) \\ \qquad \left.-T(P_d-P_s)\cos\theta_2\right]H \end{cases}$$

where,

$$\begin{cases} N = 1,\ i_1 = 2j-1,\ i_2 = 2j, \text{ and } \theta_2 = \theta^* \quad (\theta_o \leqq \theta^* < \pi) \\ N = 2,\ i_1 = 2j,\ i_2 = 2j+1, \text{ and } \theta_2 = \pi-\theta^* \quad (\pi \leqq \theta^* < 2\pi) \\ N = 1,\ i_1 = 2j+1,\ i_2 = 2j+2, \text{ and } \theta_2 = 2\pi-\theta^* \\ \qquad\qquad (\pi \leqq \theta^* \leqq 2\pi+\theta_o) \end{cases} \qquad \ldots\ldots\ldots\ldots\ldots\ldots (15)$$

In Eq.(15), $\theta^* = \theta-\theta_o$, and j means the j-th semicircle from outside. And the radial force, $Fc(\theta)$, is given by

$$Fc(\theta) = \sqrt{\{Fcx(\theta)\}^2+\{Fcy(\theta)\}^2} \qquad (16)$$

The calculated results of Eqs.(9) ~ (16) are shown in Fig.6 ~ 8. Fig. 6 shows that the upward thrust is very large, when the space in the housing below the end plate of the orbiting scroll is provided with discharge pressure. It is undesirable that this large thrust force results in increasing wear of the sliding surface between the orbiting scroll and the fixed scroll.

Fig. 7 shows that the absolute value of the downward thrust decreases to about 1/5 of the absolute value of the upward thrust shown in Fig. 6, when the space in the housing below the end plate of the orbiting scroll is provided with suction pressure. But the orbiting scroll is pressed in the axial direction to separate it from the fixed scroll. It is undesirable that this downward thrust in the leakage of the pressurized gas.

So, we developed the original method as follows.

PRESSURE CHAMBER FORMED BETWEEN THE ORBITING SCROLL AND THE FRAME

The pressure chamber of the developed prototype is shown in Fig. 9. The space in the housing below the end plate of the orbiting scroll is provided with suction pressure. The annular member which is provided with the pressure chamber is formed between the end plate of the orbiting scroll and the flame. The orbiting scroll is pressed in the axial direction to the fixed scroll by an upward force which is caused by introducing the high pressure gas into the pressure chamber. This upward force is given by

$$Ft(\theta) = -\sum_{i=1}^{m} \{Pi(\theta)\cdot Ati(\theta)\}\cdot Ps + \{\sum_{i=1}^{m} Ati(\theta)\}\cdot Ps + A_h(P_h - Ps) \quad \cdots\cdots\cdots (17)$$

where A_h is the area of the pressure chamber and P_h is the pressure of the pressure chamber.

EXPERIMENTS

The refrigerant capacity was measured with a gas calorimeter developed by us, and input power of the compressor was measured with a Wattmeter.

Pressure of Pressure Chamber

The performance of the scroll compressor was measured for the various pressures of the pressure chamber.

Fig. 10 shows the experimental results. In this figure, the thrust force which is calculated by Eq.(17) is the axis of abscissa, and the superscript * shows the value of the basis. When the thrust force ratio is about 1.4, the volumetric efficiency ratio becomes maximum, the input ratio becomes minimum, and the overall efficiency ratio becomes maximum. The reasons were thought to be as follows.

As the thrust force is getting low; (1) The orbiting scroll is inclining while it is orbiting. So, the axial clearance in wrap increases. The capacity decreases, since the leakage from the compression chamber to the suction side increases due to the axial clearance. (2) Since the leakage gas from the inner compression chamber to the outer compression chamber is re-compressed, the input increases.

The inclination of the orbiting scroll was clarified by the next experiment.

Measurement of Orbiting Scroll Behavior

The transducer mounting and the measuring system for measuring the orbiting scroll behavior is shown in Fig. 11. The orbiting scroll behavior was measured by an eddy current probe mounted in the fixed scroll. The crank angle was also detected with the use of an eddy current probe mounted in the flame. These signals were amplified and stored in the multi-channel wave memorizer. After that, they were displayed on the display monitor, and memorized in the floppy disk. The measurement results are shown in Fig. 12. Where Z is the orbiting scroll displacement shown in Fig. 11, and Cz is the clearance of the end plate shown in Fig. 9. This figure shows that the orbiting scroll displacement increases in axisl direction, as the thrust force ratio decreases. So, it was confirmed that the inclination of the orbiting scroll caused deteriorating performance, as the thrust force was getting low.

As a result of these experiments, the optimum thrust force ratio is about 1.4. And it has been clarified that the discharge pressure is reasonable.

Clearances

The performance of the scroll compressor was measured for the various axial and radial clearances in scroll wrap. Fig. 13 shows the experimental results. This figure shows that the axial clearance greatly influences compressor performance, but the radial clearance doesn't influence much.

By improving the axial and radial clearances in wrap to be optimum and by using the pressure chamber, the high efficiency prototype of the scroll compressor has been developed which has 9% higher overall effiency and has 30% higher volumetric efficiency than a reciprocating compressor. (See Table 1)

CONCLUSIONS

(1) The basic equations for the compression chamber volume, the forces acting on the orbiting scroll were obtained in the case in which a series of semi-circles were utilized for the scroll walls.

(2) The original method, which utilized the discharge pressure against the thrust force acting on the orbiting scroll, was suggested, and it has been clarified that this method is practical.

(3) By improving the axial and radial clearances in wrap to be optimum and by using the above mentioned method, the prototype of the scroll compressor, which has 9% higher overall efficiency and 30% higher volumetric efficiency than a reciprocating compressor, has been developed.

REFERENCES

(1) Morishita, E. et al, "SCROLL COMPRESSOR ANALYTICAL MODEL", '84 Purdue Comp. Tech. Conf.

(2) Morishita, E. et al, "GEOMETRICAL THEORY OF SCROLL COMPRESSOR (in Japanese)", Turbomachine, Vol. 13, No. 4, Apr. '85.

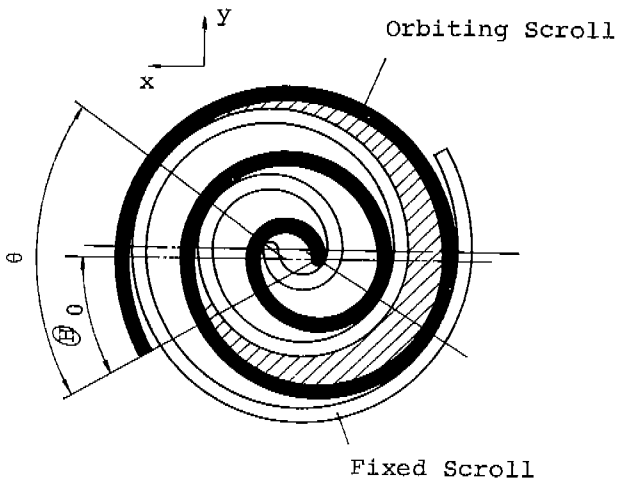

(a) $0 \leqq \theta < \pi$

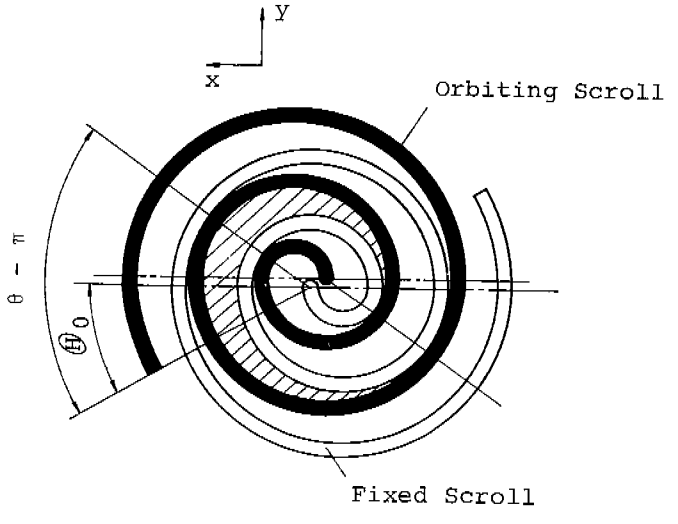

(b) $\pi \leqq \theta \leqq 2\pi$

Fig. 1 Compression Chamber

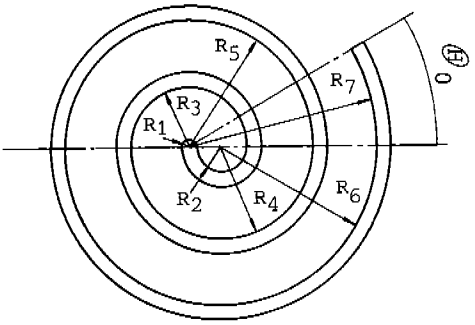

Fig. 2 Illustration of Rj

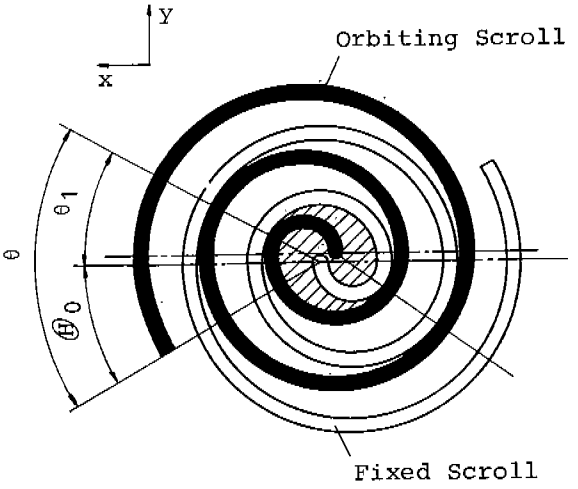

Fig. 3 Inmost Chamber

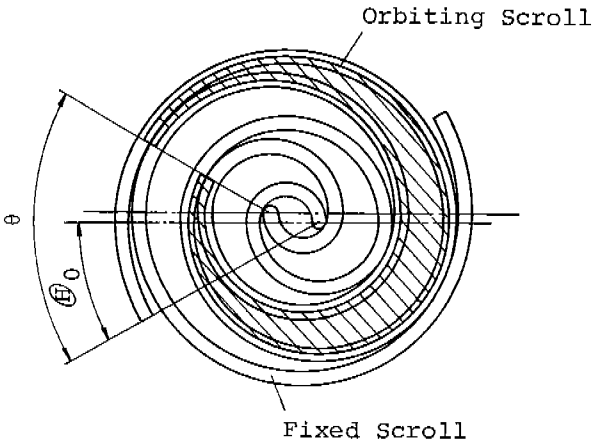

Fig. 4 Illustration of Ati (θ)

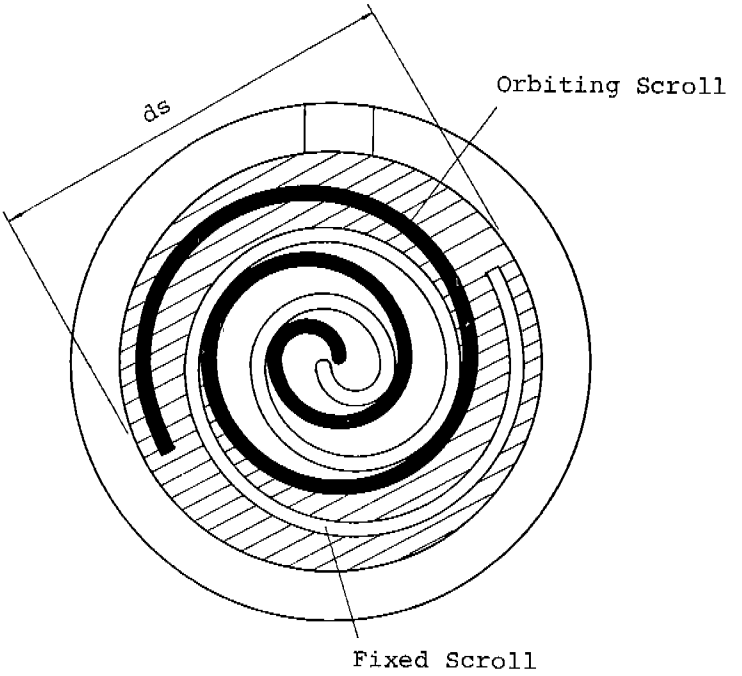

Fig. 5 Area of Suction Chamber

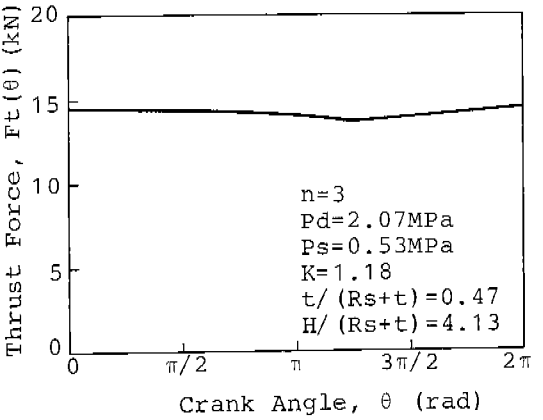

Fig. 6 Thrust Force Acting on Orbiting Scroll
(When Pd is acting below the end plate of the orbiting scroll)

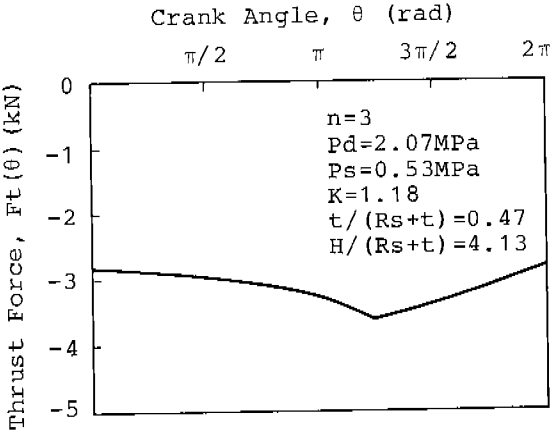

Fig. 7 Thrust Force Acting on Orbiting Scroll
(When Ps is acting below the end plate of the orbiting scroll)

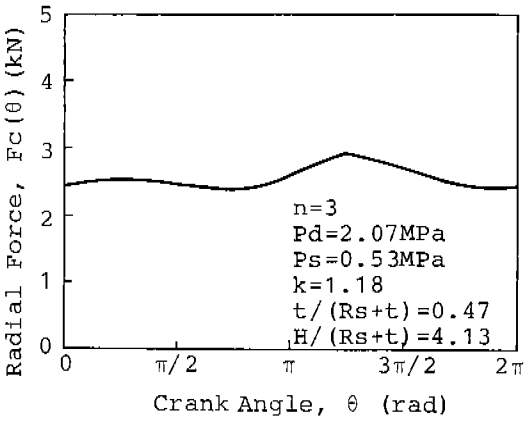

Fig. 8 Radial Force Acting on orbiting Scroll

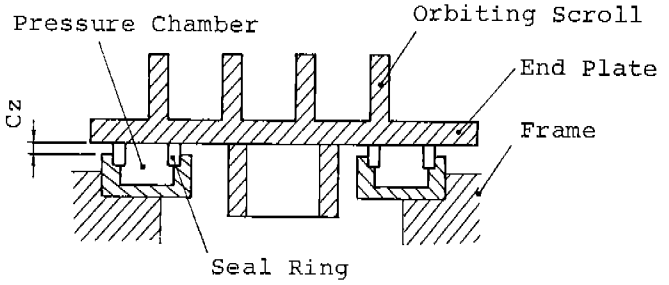

Fig. 9 Section of Pressure Chamber

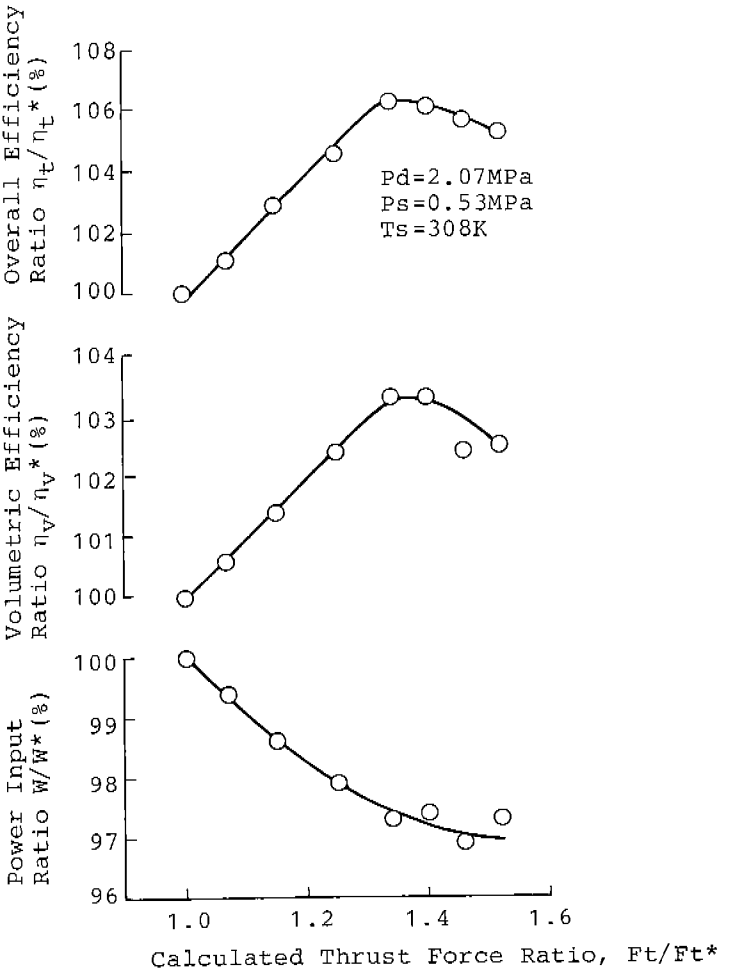

Fig. 10 Pressure of Pressure Chamber Effects on Compressor Performance

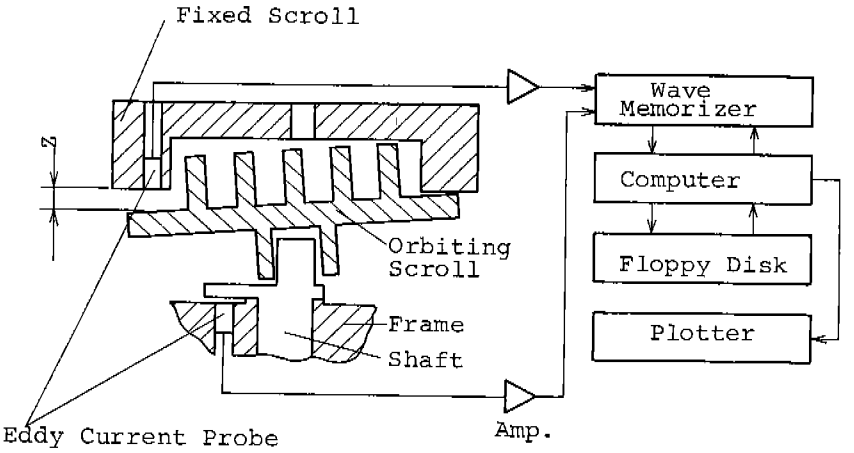

Fig. 11 Measuring System of Orbiting Scroll Behavior

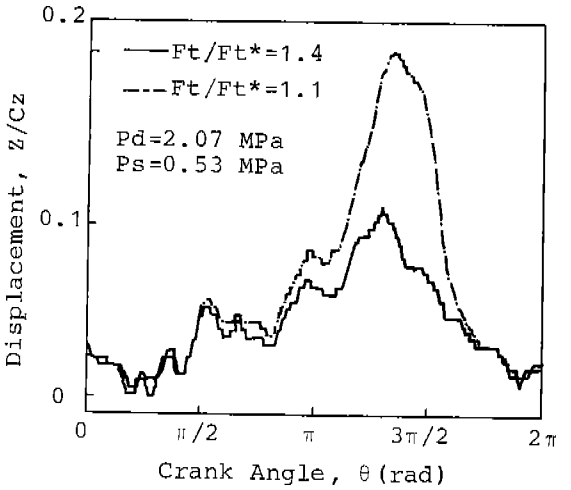

Fig. 12 Orbiting Scroll Displacement in Axial Direction

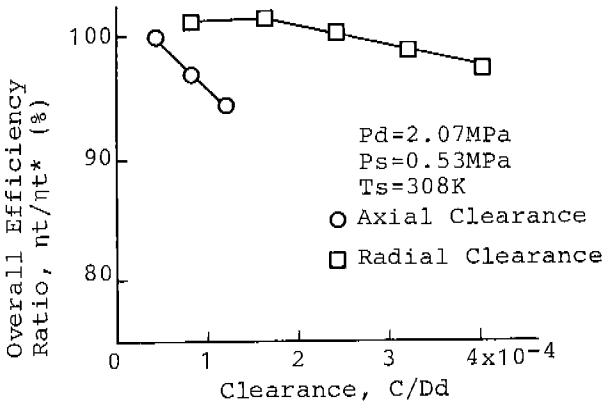

Fig. 13 Radial and Axial Clearance Effects on Compressor Performance

Table 1 Performance of Prototype Compared with Reciprocating

	RECPRO-CATING	SCROLL
Power Input Ratio	1	0.94
Volumetric Efficiency Ratio	1	1.30
Overall Efficiency Ratio	1	1.09

(Efficiency of reciprocating compressor is taken as 1)